Ceramics International xxx (xxxx) xxx

Contents lists available at ScienceDirect

Ceramics International

journal homepage: www.elsevier.com/locate/ceramint

Structural and electrodynamic characteristics of the spinel-based composite system

A.V. Trukhanov [a,b,**], D.I. Tishkevich [a,b], A.V. Timofeev [a], V.A. Astakhov [a], E.L. Trukhanova [a,b], A.A. Rotkovich [b,*], Yuan Yao [c], D.S. Klygach [d], T.I. Zubar [b], M.I. Sayyed [e,f], S.V. Trukhanov [a,b], V.G. Kostishin [a]

[a] National University of Science and Technology MISiS, 119049, Moscow, Russia
[b] Scientific-Practical Materials Research Centre of NAS of Belarus, 220072, Minsk, Belarus
[c] MIIT Key Laboratory of Critical Materials Technology for New Energy Conversion and Storage, School of Chemistry and Chemical Engineering, Harbin Institute of Technology, Harbin, 150001, PR China
[d] South Ural State University, 454080, Chelyabinsk, Russia
[e] Renewable Energy and Environmental Technology Center, University of Tabuk, Tabuk, 47913, Saudi Arabia
[f] Department of Physics, Faculty of Science, Isra University, 1162, Amman, Jordan

ARTICLE INFO

Handling Editor: Dr P. Vincenzini

Keywords:
Ferrites
Spinels
Magnetic oxides
Microstructure
Electrodynamic characteristics
Electromagnetic absorption

ABSTRACT

Two- and tree-component spinel-polymer composites were produced by thermal pressing. The initial components were chosen as $CoFe_2O_4$ and $Ni_{0.4}Cu_{0.2}Zn_{0.4}Fe_2O_4$ spinels that were produced using the sol-gel method. The ratio between spinel phases varied from 1:3 to 3:1. As a polymer, fluorinated ethylene propylene was used. The concentration of the spinels in the polymer matrix was fixed at 20 mass.%. Using XRD, SEM, and high-frequency spectroscopy, the correlation between the composition, structure, and electrodynamic characteristics of composites was established. It was found that the parameters of the unit cell of ferrite fillers do not change when filling the polymer. The RL values for the initial $CoFe_2O_4$/FEP and $Ni_{0.4}Cu_{0.2}Zn_{0.4}Fe_2O_4$/FEP were in the range of −14.5 … -24.2 dB and −10.4 … -14.1 dB, respectively, which is lower than for ferrites without a polymer matrix. The maximum values of RL (as a module) were marked for $CoFe_2O_4$/FEP. Obtained values of the reflection loss coefficient in the range of 5–10 GHz open broad perspectives for the development of materials for electromagnetic absorption and 5G technology.

1. Introduction

Complex oxides based on transition metal ions are currently of great interest. This area of study has been discussed in many articles published in notable journals. Magnetic oxides with a spinel-type structure and the general formula AFe_2O_4 ferrite-spinel (FS) are of great interest [1–3]. In addition to having a spinel structure, the naturally occurring mineral magnetite “exhibited" magnetic qualities to humanity for the first time. Today, a variety of ferrites with different magnetic and electrical properties may be created because of advancements in ferrite-spinel synthesis technologies [4–6]. As previously mentioned, AFe_2O_4 (where A^{2+} is a divalent ion) is the general chemical formula that represents the structure of ferrite spinels [3]. FS are extensively studied and utilized for plenty of purposes. The chemical composition (concentration of substituents) and microstructural characteristics of FS have a considerable influence on its optical, electrical, magnetic, and electrodynamic characteristics [7,8]. FS are materials with great potential for use in microwave devices [7], soft magnetic materials for electromechanical purposes [9], and catalytic processes [10]. Due to the broad range of practical applications, new types of materials (magnetically hard and magnetically soft composites) based on FS [11] have been actively developed and researched recently. From a fundamental perspective, this class of materials is of great interest to researchers. It is noteworthy that FS can be synthesized using a variety of techniques, allowing for diversity in structural characteristics and physico-chemical features. The most often used synthesis techniques are sol-gel [12,13] and ceramic (or solid-phase) [2]. The researchers were able to create stoichiometric and single-phase samples with different compositions by using these

* Corresponding author.
** Corresponding author. National University of Science and Technology MISiS, 119049, Moscow, Russia.
E-mail addresses: truhanov86@mail.ru (A.V. Trukhanov), rottkovich@gmail.com (A.A. Rotkovich).

https://doi.org/10.1016/j.ceramint.2024.03.241
Received 15 January 2024; Received in revised form 4 March 2024; Accepted 18 March 2024
Available online 19 March 2024

techniques. The fundamental steps of the ceramic method are mechanical mixing, heat treatment (sintering), and simultaneous grinding of the mixture's original ingredients (metal ion oxides). Heat treatment during ferritization—the creation of a phase with a spinel structure—is performed at the maximum temperature that thermodynamics allows in order to speed up diffusion processes. The main benefits of this technology are that it doesn't require expensive components, is highly manufacturable, and is simple to implement. The primary drawbacks are the initial mixture's relative heterogeneity and the potential for impurity phases to emerge during synthesis.

Nowadays, the synthesis and study of composite materials based on soft magnetic [13–15] and hard magnetic [11,16,17] ferrites is an issue that many researchers worldwide are interested in. Soft ferrites that have a structure similar to that of spinel are being intensively researched. Hard ferrites are ferrites that have a magnetoplumbite structure. As a result, it is possible to establish distinctions between various composite material types according to ferrites: 1. ceramic composites (powdered ferrites are mixed, compacted, and sintered in the form of ceramic samples) [18–20]; 2. polymer composites (powdered ferrites are introduced into the polymer matrix by dispersion in the liquid-phase medium of the matrix or by thermal pressing of powdered solid-phase mixtures) [21–23]; 3. CerMet structures (composites formed by mixing of the ceramic phase and metal powder fractions) [24–26]. All varieties of composite materials are interesting from an academic and practical viewpoint. Two sub-types of ceramic composites, particularly type No. 2, are commonly distinguished in magnetic materials: 1. "Hard-soft" composite materials [27,28]: CMs that consist of a combination of soft magnetic materials with high saturation magnetization (Ms) and low coercive force (e.g., ferrites with a spinel-type structure) and magnetically hard materials with high values of residual magnetization (Mr) and coercive force (Hc) (e.g., hexagonal ferrites); 2. "Soft--Soft" composite materials [14,13]: CMs that consist of a mixture of two magnetically soft phases. Two ways of interaction between magnetic phases can be applied in this subtype of composite material. A dipole interaction mechanism occurs when the grains of "hard-hard ferrite" or "soft-soft ferrite" interact with one another. The interaction has an exchange-coupling nature if interactions between hard-soft grains predominate. Exchange interactions and magneto-crystalline anisotropy have a major role in determining magnetization when dipole interactions are negligible. In composites with two magnetic phases, an increase in the concentration of the soft magnetic phase makes dipole interactions more prominent. The magnetic parameter values of composites alter as a result. Additionally, there may be notable changes in electrical characteristics as a result of the combining of two fractions with various electrical values. Variations in electrical and magnetic aspects, particularly magneto-crystalline anisotropy, have a significant impact on the microwave characteristics of composite materials. It's important to note that the effects seen in metamaterials, notably negative permeability values, can also be found in CerMet composites that contain metal powder in the ferrite matrix. These values have an impact on the characteristics of the composites' interaction with microwave radiation.

It must be highlighted that the results of the investigations related to the correlation between the chemical composition (concentration of the substituents), structural characteristics, and physical properties of substituted spinel ferrites have attracted great attention recently [29–33].

The goal of the investigation is to establish the correlation between chemical composition (ratio between magnetic fillers $CoFe_2O_4$ and $Ni_{0.4}Cu_{0.2}Zn_{0.4}Fe_2O_4$ in ceramic/polymer composites), evolution of microstructure, magnetic properties, and electrodynamic characteristics of spinel-based ($CoFe_2O_4$ and $Ni_{0.4}Cu_{0.2}Zn_{0.4}Fe_2O_4$) composites.

2. Experiment

The method known as sol-gel was used to synthesize composite materials (CMs) [13]. The powdered fillers of CMs were found to be $CoFe_2O_4$ (or CF) and $Ni_{0.4}Cu_{0.2}Zn_{0.4}Fe_2O_4$ (or NCZ), ferrites with a spinel-type structure (soft magnetic materials or soft magnetics). Table 1 provides information about the samples' composition.

Ternary soft-soft/polymer composite materials were synthesized by means of the thermal compression technique. As specified in Table 1, soft-soft CM samples were utilized as a magnetic ferrite filler. As a polymer matrix, powdered fluorinated ethylene propylene (FEP) was employed. One of the copolymers of hexafluoropropylene and tetrafluoroethylene is FEP. Advantages of this polymer include resistance to aging, chemical inertia, heat resistance, strength, flexibility, a low coefficient of friction, a lack of adhesion, low water absorption, and weather resistance.

There were multiple stages to the thermal pressing. A mechanical mixture of soft/soft/polymer was created at the initial step. The hangings were weighed using HR250 AZG scales in accordance with the recommended ratios of concentration between the magnetic ferrite filling (soft-soft CMs) and the matrix (FEP). For every sample of CMs soft-soft, CMs with an 80 wt% polymer (FEP) ratio and 20 wt% ferrite fillers (soft-soft) were produced. Using ethyl alcohol as a surfactant, the soft-soft and FEP powders were mixed in a porcelain mortar. The low-dimensional state of the soft-soft CM samples and the strong adhesion between the polymer FEP and ferrite powder were both noted. It is clear that electrostatics caused both of these observations. The uniform distribution of particles and the mixing of components were promoted by this situation. The color alteration served as a circumstantial indicator of how uniformly the components were distributed throughout the mixture. The final mixture was pressed in a stainless-steel mold (grade U8). At the second stage. In order to eliminate air gaps, pressure P ~1 ton was applied three times prior to pressing. For the purpose of determining the microwave characteristics within the microwave range, parallelepiped samples were created, measuring 36 × 16 mm in size and varying in thickness from 1 to 4 mm. 350 °C was the temperature under thermobaric exposure. 10 min was the exposure period.

An ADVIN POWDIX 600 diffractometer and an X-ray diffraction (XRD) study with Co-K_α radiation were used to conduct structural-phase analysis [30]. Method of scanning: point-by-point, step 0.03, angle range 2θ: 20–80°. XRD data processing was performed using the Rietveld method as part of a full-profile analysis. The XRD data's qualitative phase analysis is conducted using the "COD" database, and the data is concurrently compared with the "ICDD PDF-2″ database.

Morphologies were examined with a scanning electron microscope, the Carl Zeiss EVO 10. The research objects' particles were arranged according to size by determining the equivalent diameter. The following formula [31] was used to calculate the proportion of occupied area (P):

$$P = \frac{\pi n_i d_i^2}{4S} \quad (1)$$

Table 1
Detailed sample information: sample's number (No.); sample's acronym; sample's composition (ratio between ceramic phases and polymer concentration); and sample's density (ρ).

No.	Acronym	Composition and ceramic phase ratio	Ceram/FEP ratio, wt.%	ρ, g/cm^3
S1	CF/FP	$CoFe_2O_4$	20/80	2.39
S2	NCZ/FP	$Ni_{0.4}Cu_{0.2}Zn_{0.4}Fe_2O_4$	20/80	2.23
S3	(CF_3: NCZ_1)/FP	$CoFe_2O_4$: $Ni_{0.4}Cu_{0.2}Zn_{0.4}Fe_2O_4$ = 3:1	20/80	2.31
S4	(CF_2: NCZ_1)/FP	$CoFe_2O_4$: $Ni_{0.4}Cu_{0.2}Zn_{0.4}Fe_2O_4$ = 2:1	20/80	2.29
S5	(CF_1: NCZ_1)/FP	$CoFe_2O_4$: $Ni_{0.4}Cu_{0.2}Zn_{0.4}Fe_2O_4$ = 1:1	20/80	2.25
S6	(CF_1: NCZ_2)/FP	$CoFe_2O_4$: $Ni_{0.4}Cu_{0.2}Zn_{0.4}Fe_2O_4$ = 1:2	20/80	2.25
S7	(CF_1: NCZ_3)/FP	$CoFe_2O_4$: $Ni_{0.4}Cu_{0.2}Zn_{0.4}Fe_2O_4$ = 1:3	20/80	2.24

where d_i is the particle's size (diameter of the analogous circle), n_i is the number of particles in the i-th dimension, and S is the total area of all the particles in the image. Additionally, the hexaferrites under study were investigated via energy-dispersive X-ray spectroscopy (EDX). An Ultim Max 40 detector (Oxford Instruments, UK) equipped with AZtecLive Advanced Energy Dispersive X-ray Spectroscopy was used for the EDX investigation.

Studies of electrodynamic characteristics were carried out in the frequency range from 5 to 10 GHz using the Agilent vector circuit analyzer. The permittivity and permeability of the material were calculated using the Nicholson-Ross-Weir algorithm using S-parameters recorded as a function of frequency by the coaxial method. The impedance of the coaxial line was estimated by the following formula:

$$\dot{Z} = 60 \ln\left(\frac{D}{d}\right)\sqrt{\frac{\dot{\mu}}{\dot{\varepsilon}}} \quad (2)$$

where D is the outer diameter; d is the inner diameter of the coaxial cable; μ is the magnetic permeability (complex value); ε is the dielectric constant (complex value). The following formula determines the reflection loss (coefficient RL):

$$|\dot{R}| = 20 \lg\left(\frac{\sqrt{\frac{\dot{\mu}}{\dot{\varepsilon}}} - 1}{\sqrt{\frac{\dot{\mu}}{\dot{\varepsilon}}} + 1}\right) \quad (3)$$

Measurements of the magnetic properties were made at room temperature in a field range up to 7 T by the VSM (Liquid Helium Free High Field Measurement System).

3. Results and DISCUSSION

3.1. Structural properties

Fig. 1 shows the results of the study of the crystal structure of synthesized samples by X-ray diffraction.

Fig. 1a shows the diffraction spectra of the initial ferrite materials (CF and CNZ), which were previously synthesized by the sol-gel method. In the figure, 6–7 intense diffraction maxima can be observed, corresponding to the spinel-like structure of ferrite. The space group (SG) of the structure is *Fd-3m*. There are covalent cations (Co^{2+}, Ni^{2+}, Cu^{2+}, and Zn^{2+}) and ferric cations (Fe^{3+}) in the spinel crystal structure. These are arranged in tetrahedral (Th) and octahedral (Oh) coordinates, or in oxygen environments. The main diffraction peaks that can be observed on X-ray images correspond to the following (hkl): (202) at ~30.4°; (311) at ~35.8°; (222) at ~37.3°; (400) at ~43.3°; (422) at ~53.6°.; (511) at ~57.2°; and (440) at ~62.9°. The most intense peaks are (311), (202), and (440). The absence of other diffraction peaks not belonging to SG:*Fd-3m* for all studied CMs confirms the single-phase nature of both the initial ferrites (CF and NCZ) and the absence of any chemical interaction between the phases in S1–S7 composite materials.

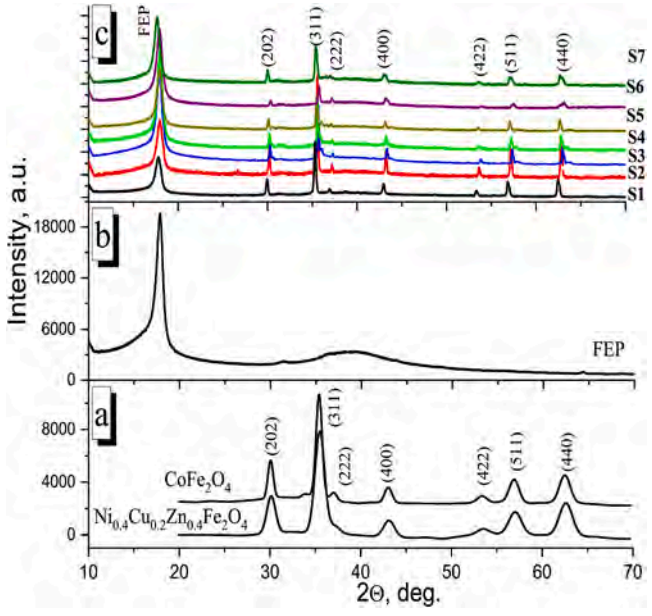

Fig. 1. XRD patterns of the (a) initial ceramic $CoFe_2O_4$ and $Ni_{0.4}Cu_{0.2}Zn_{0.4}Fe_2O_4$ samples; (b) FEP and (c) S1–S7 composites.

Fig. 1b shows the spectrum of the polymer matrix (FEP). Diffraction spectra are presented for a pure FEP polymer. The only characteristic diffraction maximum in the region of 17.9° can be noted, and there is a wide plateau in the area of 35–45°. Fig. 1c shows the diffraction spectra of samples of composite materials S1–S7. For the S1–S7 CM spectra, as well as for the initial ferrites, 6–7 intense diffraction maxima corresponding to the spinel-like structure of ferrite can be observed. Also, only peaks characteristic of FEP and initial ferrites are marked on the CM diffraction spectra. This proves that the initial CM was made up of a single phase and that the ferrite phases and the FEP polymer did not interact chemically with each other. Moreover, it can even be noted that the position of the diffraction maxima for fillers (ferrites) and polymers (FEP) corresponds to CMs, as does the preserved ratio of intensities compared with the initial compounds (CF, CNZ, and FEP). The first fact indicates the immutability of the unit cell parameter of ferrite CMs in the polymer, and the second fact indicates the absence or formation of any texture in CMs. The X-ray images were analyzed using the Rietveld method. The parameters of the unit cell (a), the volume of the unit cell (V), and the average size of the crystallite (D_{XRD}) or the average size of the coherent scattering region (CSR) of X-ray radiation (calculated using the Scherrer formula) for the initial ferrite compositions were determined. Thus, it was found that the parameter a for CF (8.3726 Å) is slightly less than for CNZ (8.4043 Å). A similar situation was noted for the volume of the unit cell (586.91 $Å^3$ for CF compared to 593.60 Å3 for CNZ). The average size of the coherent scattering region for CF (30.2 nm) was also smaller than for CNZ (41.1 nm). The processing X-ray diffraction results show that the structural properties of soft-soft CM can be passed on to a composite with a polymer without changing the crystal structure's parameters. This emphasizes the absence of any chemical interaction or mutual influence of the CM components on each other.

Fig. 2 shows SEM images and the analysis of the distribution of the average grain size in the studied samples. The analysis of the average grain size and grain size distribution for each cM sample was carried out using a standard statistical method using SmartSEM software.

According to the results of the SEM research, it is shown that the structure and distribution of the chemical elements of the pure FEP matrix are homogeneous. In CMs, there is a tendency to the formation of soft-soft powdered CM agglomerates in the FEP matrix, which is clearly visible in the distributions of chemical elements and is confirmed by SEM images.

CM S1 and S2 have a particle size distribution that is well described by the Gaussian distribution. All CM samples are characterized by similar behavior in accordance with the concentration of the initial ferrite phases. It is noted that the particles in KM S2 have a smaller size and range from 0.2 to 1.5 μm. The most probable particle size is 0.45 μm. KM S1 contains particles ranging in size from 1.0 to 2.0 μm; the most probable size is 1.65 μm. All other KM have a well-defined bimodal particle size distribution. The extremes of the Gaussian function correspond to the most probable values of each individual component. Two values of the most probable grain sizes were determined for each CM sample. It is shown that the grain size for the coarse fraction decreases monotonously from 1.65 to 1.23 μm, and the particle size of the fine fraction varies non-linearly from 0.43 to 0.47 μm. There was no obvious effect of the polymer matrix on the microstructural parameters of KM S1–S7. A similar effect of the ratio of ferrite phases in KM S1–S7 is noted.

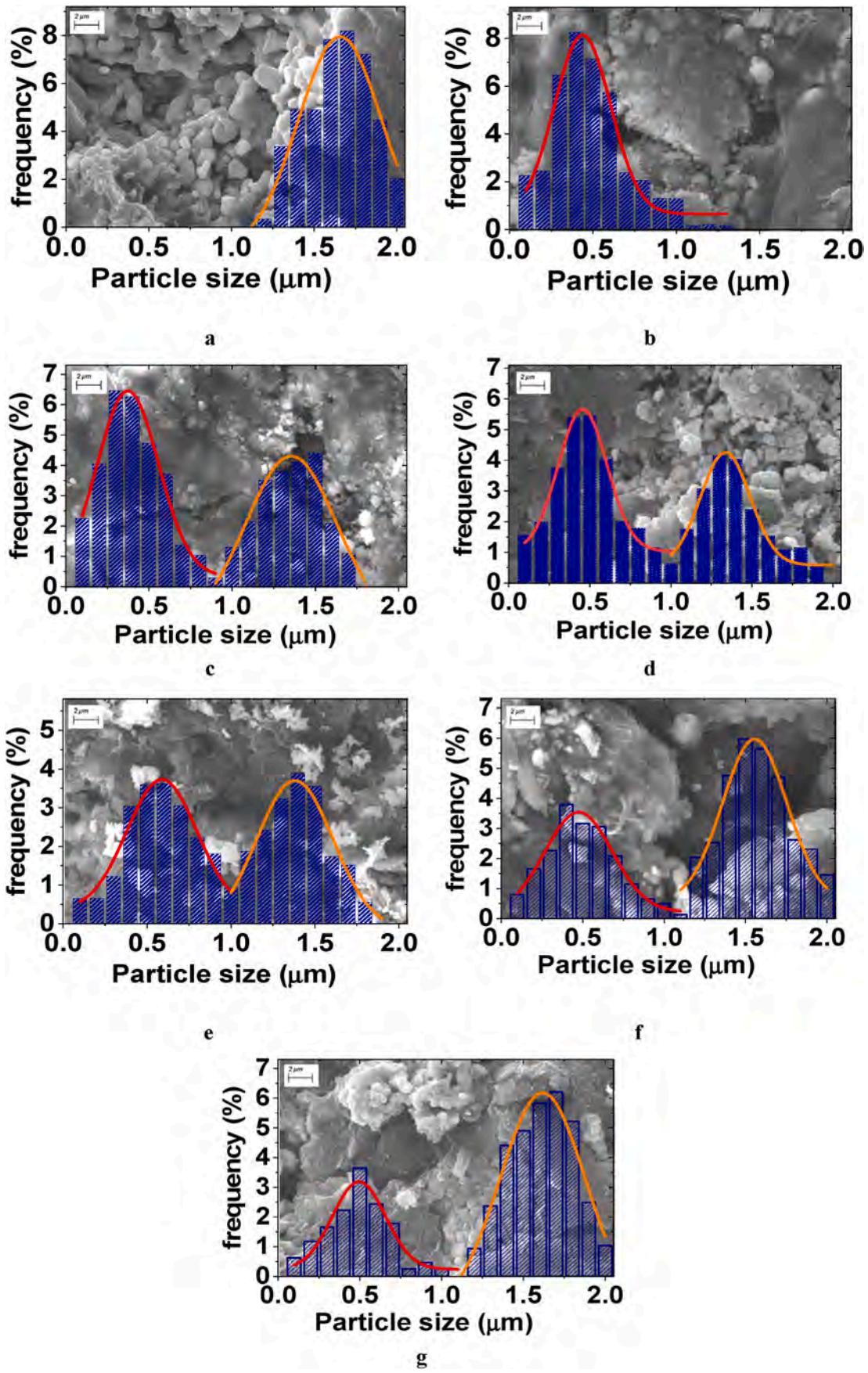

Fig. 2. SEM images and particle size distribution for (a) S1; (b) S2; (c) S3; (d) S4; (e) S5; (f) S6 and (g) S7 composites.

An increase in the NCZ content from 1:1 (S5) to 1:3 (S7) at a fixed concentration of soft-soft CMs (20 wt%) leads to a decrease in the average grain size for both small and large fractions. It's also clear that raising the concentration of CF in CMs from 1:1 (S5) to 3:1 (S3) promotes the growth of large grains that are 1–2 μm in size per CM, and raising the concentration of NCZ in CMs also contributes to the growth of grains that are 0.33–0.58 nm in size on average.

3.2. Electrodynamic characteristics

The electrodynamic characteristics were studied in the frequency range of 5–10 GHz using the Agilent vector circuit analyzer. The Nicholson-Ross-Weir algorithm was used to figure out the material's permittivity and permeability. S-parameters were recorded as a function of frequency using the coaxial method. The impedance of the coaxial line was estimated using formula (2). Reflection losses (RL coefficient) were determined by formula (3).

Fig. 3 shows the behavior of the dielectric constant (real and imaginary parts of the dielectric constant) as a function of frequency.

It is noted that for all CMs S1–S7, the values of the real part of the permeability are in the range of 5.75–2.0, which is significantly higher than the values for similar CMs but without a polymer matrix. It is shown that with increasing frequency, there is a decrease in the values of the real part of the dielectric constant (Fig. 3a). The decrease in the actual part of the dielectric constant with increasing frequency has a monotonous character.

The values of ε' for CMs S1 and S2 were in the range of 3.46–2.01 and 5.66–3.58, respectively. It should be noted that there is no synergistic effect. The values of all CMs S3–S7 were in the range between the values of ε' for CMs S1 and S2. This is explicable by the fact that the polymer matrix material makes a significant contribution to the value of CMs, whereas the ferrite filler's composition does not significantly affect the behavior of CM's microwave characteristics. The values of the imaginary part of the dielectric constant are almost an order of magnitude lower for CMs S1–S7 compared to CMs without a polymer matrix (Fig. 3b). A slight increase in the value of ε" was noted with increasing frequency. This may be due to an increase in the contribution of dipole polarization in interaction with CM, which will cause a more intense absorption of EMR energy due to an increase in electrical losses (which is explained by the influence of the polymer matrix).

Fig. 4 shows the behavior of magnetic permeability (real and imaginary parts of permeability) as a function of frequency.

It is possible to note higher μ' values of CMs S1–S7 compared to CMs without a polymer matrix. Almost all CMs showed a monotonous and insignificant decrease in the actual part of the magnetic permeability. The values of μ' for CMs S1 and S2 were in the range of 1.61–1.57 and 1.83–1.75, respectively. It should be noted that there is also no synergistic effect. The values of all CMs S3–S7 were in the range between the values of μ' for CMs S1 and S2.

The values of μ" CMs S1–S7 were significantly lower than for CMs without a polymer matrix (Fig. 4b), which is logical when forming CMs where the major part (matrix) is a non-magnetically active material (polymer). It can be assumed that in CMs based on ferrite/polymer, energy losses may increase, not due to magnetic losses but due to electrical losses. The values of μ" for the initial S1 and S2 were in the range of 0.09–0.07 and 0.13–0.07, respectively.

Fig. 5 shows the behavior of reflection energy losses (RL coefficient) as a function of frequency for S1–S7 (see Fig. 6).

The RL value for all CMs S1–S7 is negative. This corresponds to the attenuation of the reflected wave energy. It can be emphasized that all samples showed an increase in losses (modules) with increasing frequency. It can be concluded that the nature of the attenuation of reflected energy is associated with the processes of absorption of electromagnetic radiation energy to a greater extent due to electrical losses. The RL values for the initial S1 and S2 were in the range of −14.5 … -24.2 dB and −10.4 … -14.1 dB, respectively, which is lower than for CMs without a polymer matrix. It should be noted that the energy loss values for CMs S3–S7 were between the values of S1 and S2. The maximum values of RL (modulo) were marked for S1.

3.3. Magnetic characteristics

Fig. 5 shows the dependence of the magnetization vs. magnetic field strength in the range up to 7 T for S1–S7 CM. The measurements were carried out at room temperature. It can be highlighted that the maximal value of saturation magnetization (M_s) was observed for S6 (17.7 $A*m^2*kg^{-1}$). This value for composition 1:2 was higher in comparison with the initial compounds S1 (16.3 $A*m^2*kg^{-1}$) and S2 (13.6 $A*m^2*kg^{-1}$). It was observed that there was a good correlation in M_s evolution for samples with varying CF:NCZ from 3:1 (S3) to 1:1 (S5) with an increase in saturation magnetization from 8.2 $A*m^2*kg^{-1}$ to 12.5 $A*m^2*kg^{-1}$, respectively. At the same time, there was no observed correlation between M_s evolution for samples with varying CF:NCZ from 1:1 (S5) to 1:3 (S5).

The main magnetic characteristics obtained from the VSM measurements are presented in Table 2.

It must be highlighted that the main contribution to the changes in magnetic characteristics belongs to the polymer matrix and the non-homogeneity of the filler distribution in composites. This is an interesting fact that for sample S2 ($Ni_{0.4}Cu_{0.2}Zn_{0.4}Fe_2O_4$), it was observed that the H_c value was extremely low (~11 Oe), which is much lower in comparison with the ceramic bulk sample. It opens broad perspectives

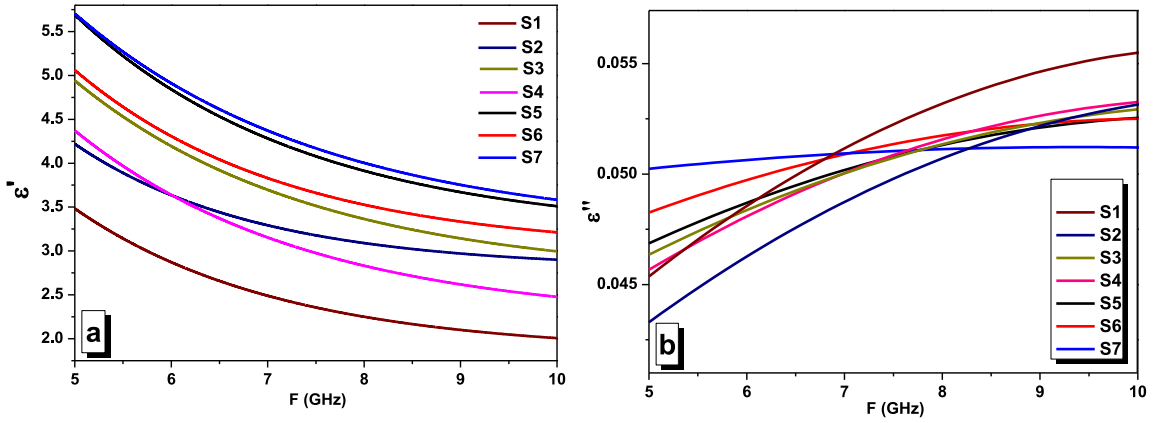

Fig. 3. Frequency dependences of the real (a) and imaginary (b) parts of the permittivity for the S1–S7 composites.

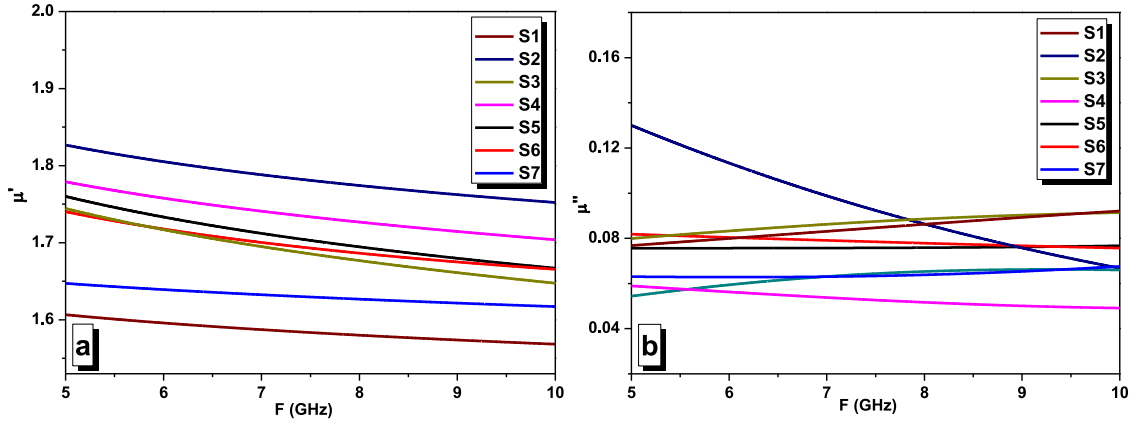

Fig. 4. Frequency dependences of the real (a) and imaginary (b) parts of the permeability for the S1–S7 composites.

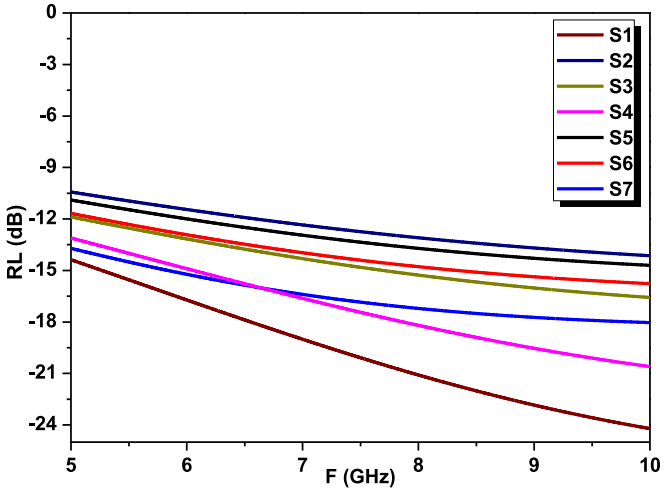

Fig. 5. Frequency dependences of the reflection losses for the S1–S7 composites.

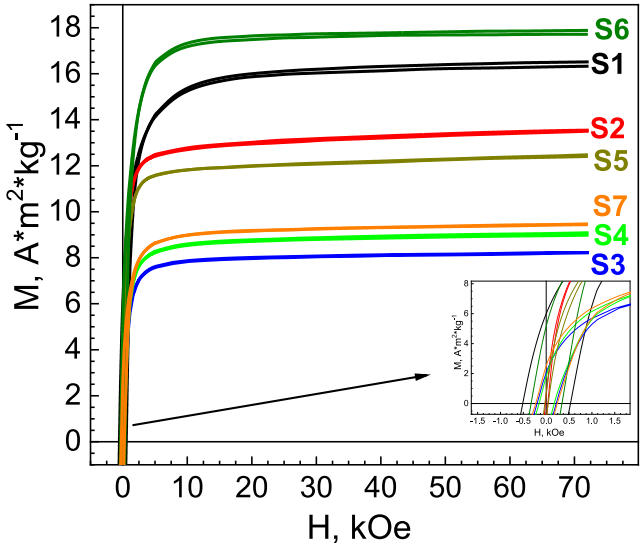

Fig. 6. Dependences of the magnetization vs. magnetic field strength for the S1–S7 composites.

Table 2
Magnetic characteristics obtained by the vibration sample magnetometry.

Magnetic characteristics	S1	S2	S3	S4	S5	S6	S7
M_s, $A*m^2*kg^{-1}$	16.3	13.6	8.2	9.0	12.5	17.7	9.54
M_r, $A*m^2*kg^{-1}$	8.3	2.7	2.4	1.6	1.2	5.2	1.2
M_r/M_s	0.51	0.20	0.30	0.18	0.09	0.33	0.13
Hc, Oe	630	11	240	170	370	290	210

for the development of functional magnetic materials for electrotechnical applications (transformers) with low magnetic losses (as cores) in the frequency range up to 100 kHz.

4. Conclusion

CMs were synthesized on the basis of soft magnetic ferrites $CoFe_2O_4$/$Ni_{0.4}Cu_{0.2}Zn_{0.4}Fe_2O_4$ (CMs soft-soft) with a variable ratio of soft magnetic phases, and CMs were synthesized on the basis of the soft magnetic KM/polymer system (CM soft-soft/FEP) with a fixed ratio of ferrite filler (20 wt%) and polymer matrix (80 wt%).

As part of the study of the structural characteristics of CMs by X-ray diffraction, it was found that the parameters of the unit cell of ferrite CM fillers do not change when filling the polymer. According to the results of the SEM research, it is shown that the structure and distribution of the chemical elements of the pure FEP matrix are homogeneous. The analysis of the grain size distribution revealed a correlation between the average grain size of CMs and the presence of two fractions in CMs: coarse (1.0–2.0 μm) belonging to CF and fine (0.2–1.5 μm) belonging to the NCZ fraction. For CMs S3–S7, the bimodal nature of the distribution is noted. It can be noted that the polymer matrix does not significantly affect the structural characteristics of the CMs.

The electrodynamic characteristics of CMs S1–S7 in the 5–10 GHz range have been studied. Based on the results of measuring the S-parameters, the values of the real and imaginary parts of the permittivity and permeability were calculated. It is shown that the reflection losses in CMs S1–S7 are due to the main contribution of electrical losses, while for CMs without a polymer matrix, the losses are due to the increasing contribution of magnetic losses. The RL values for the initial S1 and S2 were in the range of −14.5 … -24.2 dB and −10.4 … -14.1 dB, respectively, which is lower than for CMs without a polymer matrix. It should be noted that the energy loss values for CMs S3–S7 were between the values of S1 and S2. The maximum values of RL (modulo) were marked for S1. It opens broad perspectives for the development of materials for electromagnetic absorption (based on ceramic samples and ceramic composites) and 5G technology (based on ceramic:FEP composites).

Declaration of competing interest

The authors declare that they have no known competing financial interests or personal relationships that could have appeared to influence the work reported in this paper.

Acknowledgements

Investigations were supported by the Russian Science Foundation (Agreement No. 19-72-10071-П). Y.Y. acknowledges the National Natural Science Foundation of China (Grant No.U2067216).

References

[1] A. Kozlovskiy, I. Kenzhina, M. Zdorovets, Synthesis, phase composition and magnetic properties of double perovskites of A(FeM)O_{4-x} type (A=Ce; M=Ti), Ceram. Int. 45 (2019) 8669–8676.

[2] D.P. Sherstyuk, A.Yu Starikov, V.E. Zhivulin, D.A. Zherebtsov, S.A. Gudkova, N. S. Perov, YuA. Alekhina, K.A. Astapovich, D.A. Vinnik, A.V. Trukhanov, Efect of Co content on magnetic features and spin states in Ni-Zn spinel ferrites, Ceram. Int. 47 (2021) 12163–12169.

[3] V.A. Ketsko, E.N. Beresnev, M.A. Kop'eva, L.V. Elesina, A.I. Baranchikov, A. I. Stognii, A.V. Trukhanov, N.T. Kuznetsov, Specifics of pyrohydrolytic and solid-phase syntheses of solid solutions in the $(MgGa_2O_4)_x(MgFe_2O_4)_{1-x}$ system, Russ. J. Inorg. Chem. 55 (2010) 427–429.

[4] M. Almessiere, Y. Slimani, A.V. Trukhanov, A. Baykal, H. Gungunes, E. L. Trukhanova, S.V. Trukhanov, V.G. Kostishin, Strong correlation between Dy^{3+} concentration, structure, magnetic and microwave properties of the $[Ni_{0.5}Co_{0.5}](Dy_xFe_{2-x})O_4$ nanosized ferrites, J. Ind. Eng. Chem. 90 (2020) 251–259.

[5] M.A. Darwish, A.V. Trukhanov, O.S. Senatov, A.T. Morchenko, S.A. Saafan, K. A. Astapovich, S.V. Trukhanov, E.L. Trukhanova, A.A. Pilyushkin, A.S.B. Sombra, D. Zhou, R.B. Jotania, C. Singh, Investigation of AC-measurements of epoxy/ferrite composites, Nanomaterials 10 (2020) 492.

[6] M.A. Almessiere, A.V. Trukhanov, Y. Slimani, K.Y. You, S.V. Trukhanov, E. L. Trukhanova, F. Esa, A. Sadaqat, K. Chaudhary, M. Zdorovets, A. Baykal, Correlation between composition and electrodynamics properties in nanocomposites based on hard/soft ferrimagnetics with strong exchange coupling, Nanomaterials 9 (2019) 202.

[7] M. Darwish, A. Trukhanov, O. Senatov, A. Morchenko, S. Saafan, K. Astapovich, S. Trukhanov, E. Trukhanova, A. Pilyushkin, A. Sergio, B. Sombra, D. Zhou, R. Jotania, C. Singh, Investigation of AC-measurements of epoxy/ferrite composite, Nanomaterials 10 (2020) 492.

[8] P.A. Chernavskii, R.V. Kazantsev, G.V. Pankina, D.A. Pankratov, S.V. Maksimov, O. L. Eliseev, Unusual effect of support carbonization on the structureand performance of Fe/$MgAl_2O_4$ fischer–tropsch catalyst, Energy Technol. 9 (2021) 2000877.

[9] M.A. Almessiere, Y. Slimani, H. Güngünes, S. Ali, A. Manikandan, I. Ercan, A. Baykal, A.V. Trukhanov, Magnetic attributes of $NiFe_2O_4$ nanoparticles: influence of dysprosium ions (Dy^{3+}) substitution, Nanomaterials 9 (2019) 820.

[10] R. Benrabaa, H. Boukhlouf, A. Löfberg, A. Rubbens, R.-N. Vannier, E. Bordes-Richard, A. Barama, Nickel ferrite spinel as catalyst precursor in the dry reforming of methane: synthesis, characterization and catalytic properties, J. Nat. Gas Chem. 21 (2012) 595–604.

[11] O.S. Yakovenko, L.Y. Matzui, L.L. Vovchenko, V.V. Oliynyk, V.V. Zagorodnii, S. V. Trukhanov, A.V. Trukhanov, Electromagnetic properties of carbon nanotubes/$BaFe_{12-x}Ga_xO_{19}$/epoxy composites with random and oriented filler distribution, Nanomaterials 11 (2021) 2873.

[12] A.V. Trukhanov, N.A. Algarou, Y. Slimani, M.A. Almessiere, A. Baykal, D. I. Tishkevich, D.A. Vinnik, M.G. Vakhitov, D.S. Klygach, M.V. Silibin, T.I. Zubar, S. V. Trukhanov, Peculiarities of the microwave properties of hard-soft functional composites $SrTb_{0.01}Tm_{0.01}Fe_{11.98}O_{19}$-$AFe_2O_4$ (A = Co, Ni, Zn, Cu and Mn), RSC Adv. 10 (2020) 32638–32651.

[13] A.V. Trukhanov, M.A. Almessiere, A. Baykal, Y. Slimani, E.L. Trukhanova, D. I. Tishkevich, S.V. Podgornaya, E. Kaniukov, S.V. Trukhanov, Microstructure and high frequency electromagnetic parameters of the soft/soft ($CoFe_2O_4$)x: $(Ni_{0.4}Cu_{0.2}Zn_{0.4}Fe_2O_4)_y$ nanocomposites, RSC Adv. 12 (2022) 34020–34027.

[14] M.A. Almessiere, S. Güner, Y. Slimani, M. Hassan, A. Baykal, M.A. Gondal, U. Baig, S.V. Trukhanov, A.V. Trukhanov, Structural and magnetic properties of $Co_{0.5}Ni_{0.5}Ga_{0.01}Gd_{0.01}Fe_{1.98}O_4/ZnFe_2O_4$ spinel ferrite nanocomposites: comparative study between sol-gel and Pulsed Laser Ablation in Liquid approaches, Nanomaterials 11 (9) (2021) 2461.

[15] M.A. Almessiere, B. Ünal, A. Baykal, I. Auwal, Y. Slimani, A. Manikandan, A. V. Trukhanov, Investigation on electrical and dielectric properties of hard/soft spinel ferrite nanocomposites of $CoFe_2O_4/(NiSc_{0.03}Fe_{1.97}O_4)_x$, Vacuum 194 (2021) 110628.

[16] M.A. Almessiere, B. Ünal, S. Ali, A. Baykal, Y. Slimani, A.V. Trukhanov, One pot synthesis of Hard/soft $SrFe_{10}O_{19}/_x(Ni_{0.8}Zn_{0.2}Fe_{1.8}Cr_{0.2}O_4)$ nanocomposites: electrical features and reflection losses, Ceram. Int. 48 (17) (2022) 25390–25401.

[17] M.A. Almessiere, B. Ünal, A. Baykal, I. Auwal, Y. Slimani, A. Manikandan, A. V. Trukhanov, Investigation on electrical and dielectric properties of hard/soft spinel ferrite nanocomposites of $CoFe_2O_4/(NiSc_{0.03}Fe_{1.97}O_4)_x$, Vacuum 194 (2021) 110628.

[18] D. Bochenek, P. Niemiec, A. Chrobak, G. Ziółkowski, A. Błachowski, Magnetic and electric properties of the lead free ceramic composite based on the BFN and ferrite powders, Mater. Char. 87 (2014) 36–44.

[19] D. Bochenek, P. Niemiec, R. Skulski, A. Chrobak, P. Wawrzała, Ferroelectric and magnetic properties of the PMN-PT-nickel zinc ferrite multiferroic ceramic composite materials, Mater. Chem. Phys. 157 (2015) 116–123.

[20] P.P. Mohapatra, S. Ghosh, A. Jain, S. Aich, P. Dobbidi, Rare earth substituted lithium ferrite/carbon black ceramic composites for shielding electromagnetic radiation, J. Magn. Magn Mater. 573 (2023) 170678.

[21] A. Chandra Anjana, Facile synthesis and characterization of polymer composites with cobalt ferrite and biomass based activated carbon for microwave absorption, Mater. Today Commun. 37 (2023) 107397.

[22] S.K. Godara, S. Kaur, V. Bhasin, V.K. ChalotraSuman, A. Verma, J. Prakash, A. Kandwal Himanshi, 10 - antimicrobial and antibacterial applications of ferrites and their polymer composites, Magnetic Nanoferrites and their Composites (2023) 207–235.

[23] S. Kumar, P. Kumar, R. Gupta, V. Verma, Electromagnetic interference shielding behaviors of in-situ polymerized ferrite-polyaniline nano-composites and ferrite-polyaniline deposited fabrics in X-band frequency range, J. Alloys Compd. 862 (2021) 158331.

[24] R. Li, A. Feng, J. Zhao, X. Pan, G. Zhang, Y. Zhu, C. Chen, Study on process optimization of WC-Ni60A cermet composite coating by laser cladding, Mater. Today Commun. 37 (2023) 107400.

[25] Y. Belokon, O. Hrechanyi, T. Vasilchenko, D. Krugliak, Y. Bondarenko, Development of composite materials based on TiN–Mo cermets during thermochemical pressing, Int. J. Lightweight Mater. Manuf. 6 (4) (2023) 508–511.

[26] M. Zhezhu, A. Vasil'ev, M. Yaprintsev, O. Ivanov, V. Novikov, Effect of spark plasma sintering temperature on microstructure and thermoelectric properties of the cermet composites consisting of $Bi_2Te_{2.1}Se_{0.9}$ matrix and Co@$CoTe_2$ inclusions, J. Solid State Chem. 305 (2022) 122696.

[27] S. Lucarini, M. Hossain, D. Garcia-Gonzalez, Recent advances in hard-magnetic soft composites: synthesis, characterisation, computational modelling, and applications, Compos. Struct. 279 (2022) 114800.

[28] D. Li, F. Wang, A. Xia, L. Zhang, T. Li, C. Jin, X. Liu, A facile way to realize exchange coupling interaction in hard/soft magnetic composites, J. Magn. Magn Mater. 417 (2016) 355–358.

[29] K. Sakthipandi, K. Kannagi, A. Hossain, Effect of lanthanum doping on the structural, electrical, and magnetic properties of $Mn_{0.5}Cu_{0.5}La_xFe_{2-x}O_4$ nanoferrites, Ceram. Int. 46 (11) (2020) 19634–19638. Part B.

[30] A. Hossain, A.S. Volegov, K. Sakthipandi, E.A. Kiselev, V.A. Cherepanov, E. A. Mukhanova, A.V. Soldatov, Tuning of the optical and magnetic properties of $Nd_2Ni_{1-x}Co_xMnO_{6-\delta}$ ($0.2 \leq x \leq 0.5$) perovskite by cobalt doping, Ceram. Int. 49 (17) (2023) 29229–29236. Part B.

[31] R.R. Kanna, K. Sakthipandi, A.S. Kumar, N.R. Dhineshbabu, S.M. Seeni Mohamed Aliar Maraikkayar, A.S. Afroze, R.B. Jotania, M. Sivabharathy, Synthesis of dysprosium/Mn–Cu ferrite binary nanocomposite: analysis of structural, morphological, dielectric, and optomagnetic properties, Ceram. Int. 46 (9) (2020) 13695–13703.

[32] R.R. Kanna, K. Sakthipandi, A.S. Kumar, N.R. Dhineshbabu, S.M. Seeni Mohamed Aliar Maraikkayar, A.S. Afroze, R.B. Jotania, M. Sivabharathy, Synthesis of dysprosium/Mn–Cu ferrite binary nanocomposite: analysis of structural, morphological, dielectric, and optomagnetic properties, Ceram. Int. 46 (9) (2020) 13695–13703.

[33] K. Sakthipandi, B.G. Babu, G. Rajkumar, A. Hossian, M.S. Raghavan, M.R. Kumar, Investigation of magnetic phase transitions in $Ni_{0.5}Cu_{0.25}Zn_{0.25}Fe_{2-x}La_xO_4$ nanoferrites using magnetic and *in-situ* ultrasonic measurements, Phys. B: Condenser 645 (2022) 414280.